

Effect of Chemical Etching of Substrates on the Properties of Sb_2S_3 Thin Films

Fethi Aousgi

Photovoltaic Laboratory, Centre for Research and Technology Energy (CRTE_n), Borj Cédria 2050 Hammam-Lif- Tunisia

Mounir Kanzari

Photovoltaic and Semiconductor Materials Laboratory, ENIT, Tunisia

Abstract

In this work, we carried out a chemical etching on glass substrates, initially cleaned, with a solution containing hydrofluoric acid buffered with ammonium fluoride and water at different concentrations from 0 to 100 % to have an isotropic etching. The aim of this chemical etching is to create a textured surface on glass substrates, which affect the surface roughness of thin films. So, in order to achieve better photovoltaic properties Sb_2S_3 thin films have been deposited on etched glass substrates by vacuum thermal evaporation technique at substrate temperature $T_s = 300$ K. The total and diffuse reflection spectra determined in the spectral range 300 –1800 nm using UV-Vis-NIR spectrophotometer allow us to extract the surface roughness of the Sb_2S_3 films. It has been shown that the surface roughness of etched glass substrates vary greatly depending on the F^- ions concentration of the solution and the etching time. This procedure to grow highly oriented Sb_2S_3 thin films is very important since we know that well crystallization and orientation of the films affects the solar cells conversion efficiency.

1. Introduction

Recently, Sb_2S_3 is a member of V2-VI3 semiconductor materials family. In recent years, a large number of studies have been devoted to the physical properties of chalcogenides thin films due to their wide applications in optoelectronic devices [1, 2]. Among the available chalcogenides, pure and doped Sb_2S_3 thin films are used in solar energy conversion, thermoelectric cooling technologies and as photoconductive target for vidicon type of television camera [3, 4]. Due to these potential applications, it is fundamental to study in detail the structural, electrical and optical properties of this material.

Recently, researchers become interested in producing this material in thin film form. In particular, most of the works give attention to the structural and electrical properties of the Sb_2S_3 material. Sb_2S_3 thin films has been grown using several methods [5, 6] as the chemical bath

deposition [7, 8], the sol-gel method [9], vacuum evaporation method [10, 11].

One way to improve the efficiency of solar cells is the texturing of the surfaces of substrates on which thin films are deposited and this in order to inhibit the reflection of sunlight. Currently, a versatile solution are used for burning and more common for etching glass substrates is the solution of potassium oxide KOH [12]. For better performance of the cell, new techniques in the process of texturing have been developed. For example, the wet etching was used for the modification of surface of glasses for the electronic applications [13].

The aim of this work is the study the effect of the surface texturing of the substrate on the properties of the Sb_2S_3 thin films. We present results relating to the structural and optical properties of amorphous antimony sulfide thin films deposited on rough substrates made by the thermal evaporation method. The glass substrates were chemically etched by a solution of NH_4HF . The analyses of these properties depend strongly of the $[F^-]$ concentration.

2. Experimental procedures

The chemical cleaning, also called wet etching, makes itself by chemical attack in aqueous solution, acidic or basic solution partially diluted, the more used solution is the hydrofluoric acid (HF), in some cases stamped by the fluoride of ammonium (NH_4F), this solution is named in the literature (BOE: Buffered Oxide Etch) [14].

We choose a solution of hydrofluoric acid stamped by the ammonium fluoride and water ($HF/NH_4F/H_2O$) permitting to have an isotropic reaction. The aim of this reaction is to create a superficial profile, a texturing on the glass substrates which influences the roughness, the microstructure, the adhesion and therefore, the physical and chemical properties of the layers. So, we prepare a set of solutions having different concentration of the anion (F^-), by varying the factor of dilution (d) from 0% to 100% of acid (the volume ratio of HF/H_2O).

Using the texturing glass substrates, Sb_2S_3 thin films were deposited by single source thermal evaporation method [7]. Crushed powder of the Sb_2S_3 ingot was used as raw material for the thermal evaporation and a Tantale crucible was used as evaporator source. The pressure of the chamber during evaporation was about 10^{-6} Torr. The substrate temperature $T_s = 300$ K was measured using a Chromel–Alumel thermocouple in contact with substrate surface. The obtained films adhere well to the substrates.

The structure of the Sb_2S_3 thin films was determined by means of X-ray diffraction (XRD) using a D8 Advance diffractometer with $\text{CuK}\alpha$ radiation ($\lambda=1.5418$ Å). The surface morphology was carried out using a scanning electron microscope (type Philips XL30) and the roughness of the films were examined by means of atomic force microscopy (AFM) type Veeco model D3100. The optical characteristics were determined at normal incidence in the spectral range 300 to 1800 nm using a Shimadzu UV/Vis/NIR spectrophotometer. The film thicknesses were found to be in the range 470–650 nm. The conductivity type of the Sb_2S_3 thin films was determined by the hot probe method. All the films are highly compensated.

3. Results and discussion

3.1. Structural and morphological properties

X-ray diffractograms have been obtained for all the samples before and after annealing. In figure 1, Sb_2S_3 thin films deposited on substrate etched at different concentrations of the $[\text{F}^-]$ were presented. It can be observed that the samples obtained after evaporation were globally amorphous. Those samples deposited at temperature $T_s = 300$ K present similar spectra to the above samples but with a slight decrease for the rough layers.

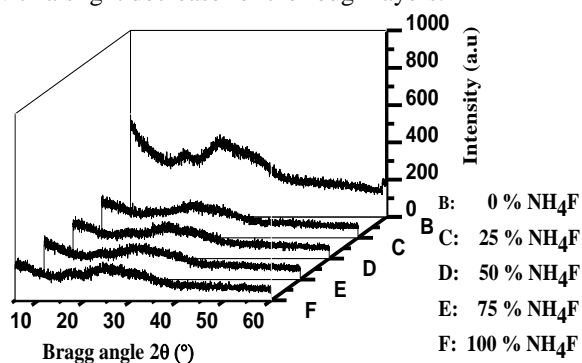


Figure 1. XRD patterns of Sb_2S_3 thin films as-deposited with different F^- % concentration

The micrographs in figure 2 show the surface states of Sb_2S_3 layers deposited on a substrate slightly attacked (25 % figure 2.a) and strongly attacked (100 % figure 2.b) by the acid solution. We see clearly the important effect of the concentration of attack substrates on the growth of layers of Sb_2S_3 material. The material is adhering to a substrate attacked.

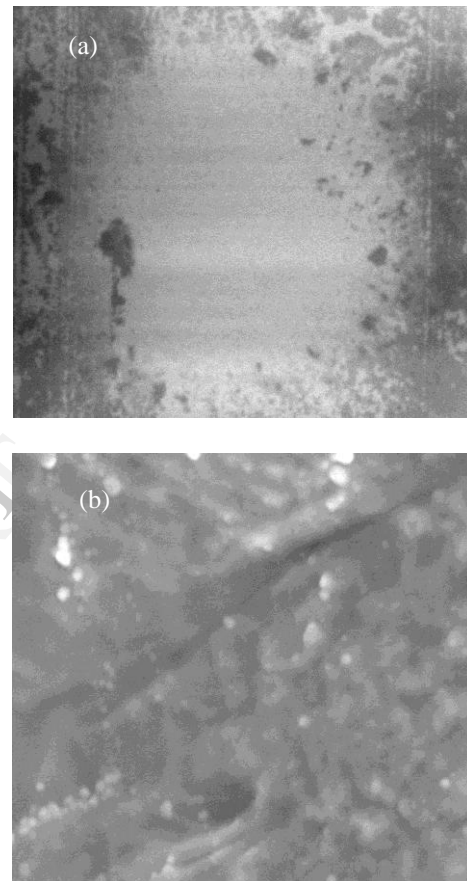


Figure 2. SEM Micrographs of Sb_2S_3 thin films as-deposited with different F^- % concentration: (a) for 25 % and (b) for 100 %.

We studied the surface morphologies of the Sb_2S_3 films by Atomic Force Microscopy (AFM). Figure 3 shows the AFM images of samples. The measured Rms is given in table 1. It is clear from the table that the average roughness decreases by increasing the concentration of F^- ions. The root mean square (Rms) values of surface roughness were found between 22.86 and 6.84 nm.

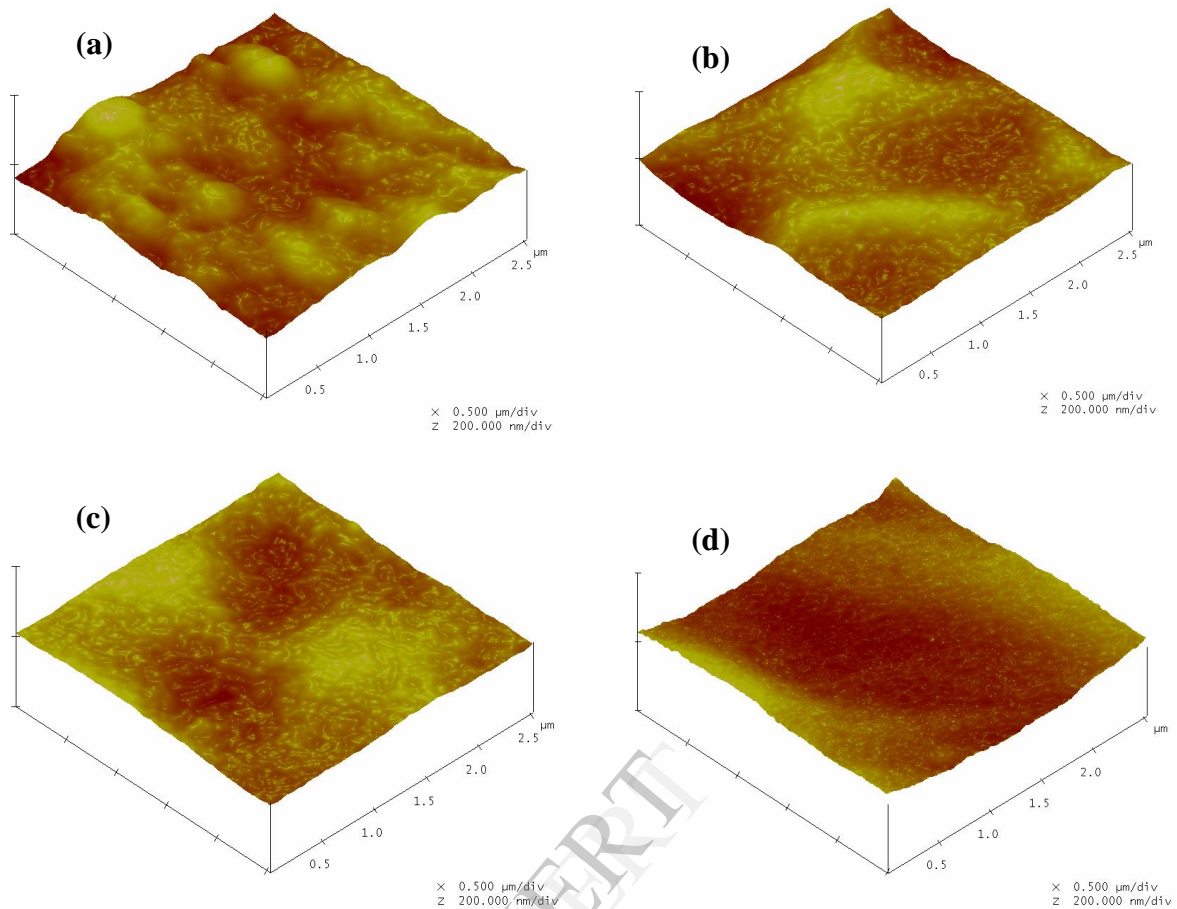


Figure 3. AFM Micrographs of Sb_2S_3 thin films as-deposited with different F^- % concentration: (a) for 25 %, (b) for 50 %, (c) for 75 % and (d) for 100 %.

3.2. Optical properties

3.2.1 Roughness of texturing glass substrates

Figure 4 shows the spectra of the total reflection and diffuse of the texturing glass substrates. These spectra show an increase in the diffuse reflection with the concentration of F^- ions. However, there was a slight decrease in total reflection.

To calculate the surface roughness of the films deposited on texturing glass substrates, we applied the following expression [15];

$$\frac{R_T}{R_s} = \exp\left[-\left(\frac{4\pi\sigma}{\lambda}\right)^2\right] + \left[1 - \exp\left[-\left(\frac{4\pi\sigma}{\lambda}\right)^2\right]\right] \times \left[1 - \exp\left[-\left(\frac{\beta\pi\sigma}{u\lambda}\right)^2\right]\right] \quad (1)$$

where;

R_S is the specular reflection and R_T is the total reflection,

R_S : the specular reflection corresponds to a smooth surface; the roughness is almost zero,

σ and u : are the average roughness of the irregularities respectively the highest and the lowest,

λ : is the wavelength of the incident radiation,

β : is half the acceptance angle of the measuring instrument.

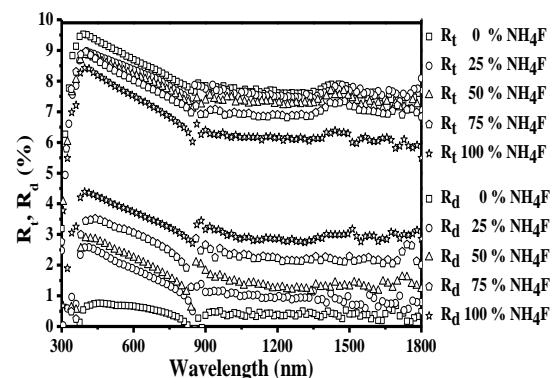


Figure 4. Total and diffuse reflection spectra of the texturing glass substrates.

The total reflection R_T can be written as the sum of R_S and R_{diff} (diffuse reflection). The first term of Eq. (1) describes the coherent part of the reflection, while the second term represents the incoherent part. The second term can be neglected and the expression is simplified to a new expression, where

C is a constant from the spatial fluctuations of the optical constants [15]:

$$\text{Ln}\left(\frac{R_T}{R_S}\right) = -\frac{(4\pi\sigma)^2}{\lambda^2} + C \quad (2)$$

The slope of $\text{Ln}(R_T/R_S)$ versus $(1/\lambda^2)$ gives the surface roughness of texturing glass substrates (Table 1).

Table 1 Roughness of texturing glass substrates and Sb_2S_3 layers at different HF concentration.

Roughness σ (nm)	Concentration HF (%)					
	0	10	25	50	75	100
Glasses	0	1.95	5.35	8.28	10.69	14.92
Sb_2S_3 layers (AFM)	22.86	17.23	12.65	10.85	8.33	6.84
Sb_2S_3 layers (calculate)	23.54	17.85	13.75	9.31	5.45	5.72

We studied the variation this roughness as a function of the concentration of [F]. According to the shape of the curve (Figure 5.a), we note that roughness strongly increases by increasing the [F] concentration.

3.2.2 Roughness calculation of the Sb_2S_3 layers

By the same procedure described above, we represent the curves of $\text{Ln}(R_T/R_S) = f(1/\lambda^2)$ [18] to obtain the roughness σ of the Sb_2S_3 layers deposited on texturing glass substrates (Table 1). According to the shape of the curve (Figure 5.b), we note that the roughness strongly decrease by increasing the [F] concentration. These results confirm the results found by the analysis of surface morphologies of the Sb_2S_3 films analyzed by AFM. In addition we note that the roughness's of the Sb_2S_3 layers are higher than those of the texturing glass substrates for the concentration of [F] less than 50 mmol.l^{-1} (Figure 5). After what the roughness's of the texturing glass substrates

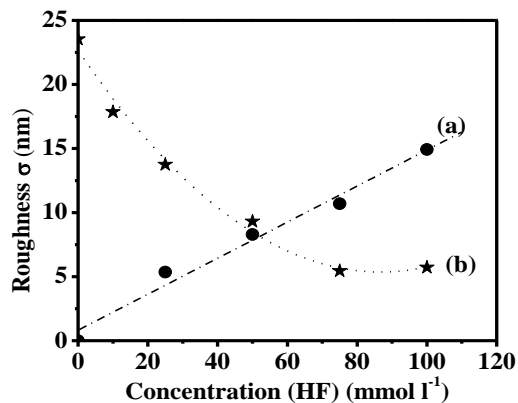


Figure 5. Roughness of attacked (a): glasses and (b): Sb_2S_3 layers with different F⁻ % concentration.

3.2.3 Optical transmission and reflection spectrum

It can be seen that for deposited Sb_2S_3 thin films, the transmittance decreases when the [F] concentration increases. This decrease becomes more important at the strong concentration of [F] (Figure 6.a). On the other hand, the reflections increase when the [F] concentration increases (Figure 6.b). This feature can be explained by the increase of roughness with the concentration that can be responsible for the anomalous decrease of optical transmittance. Also, an increase of grain boundaries with the concentration is at the origin of the destructive interference and as a consequence of the decrease of optical transmittance.

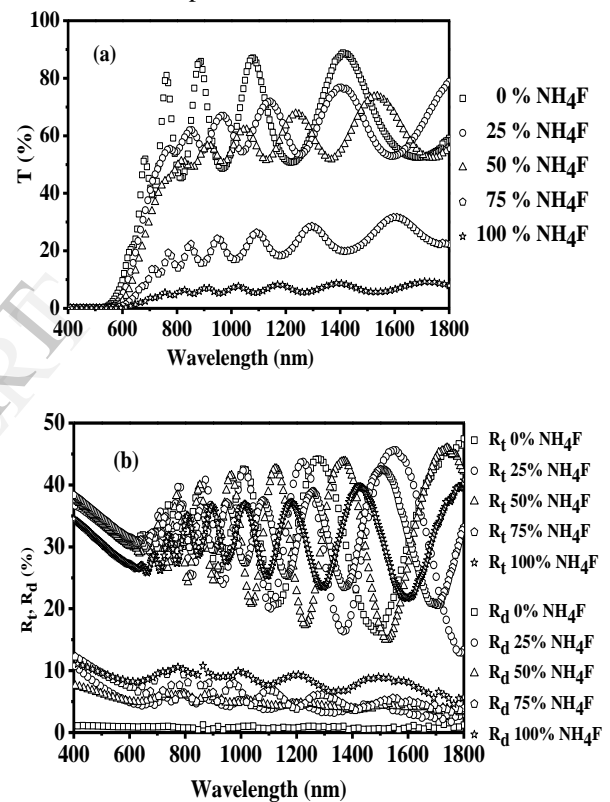


Figure .6 Transmission and reflection spectra for as-deposited Sb_2S_3 thin films with different F⁻ % concentration: (a) transmission (b) total and diffuse reflection.

3.2.4 Absorption coefficients

The variation of the absorption coefficient was calculated by the following relation [16]:

$$\alpha = \frac{1}{d} \text{Ln}\left[\frac{(1-R)^2}{T}\right] \quad (3)$$

where d is the film thickness, R and T are the reflection and transmission coefficients, respectively. The absorption coefficient α evaluated from the measurements of optical transmission and reflection through the thin film is shown in figure

7. Relatively high absorption coefficients between 10^4 cm^{-1} and 10^6 cm^{-1} were found.

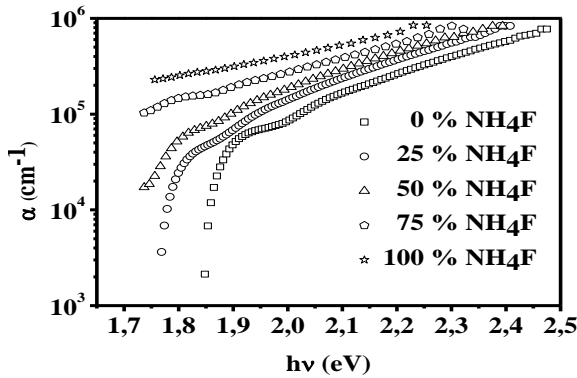


Figure 7. Absorption coefficients of Sb_2S_3 thin films with different F⁻ % concentration.

Plotting $(\alpha h\nu)^2$ versus photon energy, $h\nu$, gives way to two direct allowed transition E_{g1} and E_{g2} as observed in figure 8. The first energy gap E_{g1} is related to the direct optical transition whereas the second E_{g2} confirms the amorphous phase of the film.

Table 2 Direct energy gap E_g and Thickness of Sb_2S_3 layers at different HF concentration.

Concentration HF (%)	0	10	25	50	75	100
Thickness (nm)	600	589	602	562	536	600
E_{g1} (eV)	1.86	1.78	1.76	1.70	1.65	1.86
E_{g2} (eV)	1.98	1.87	1.85	1.80	1.79	1.98

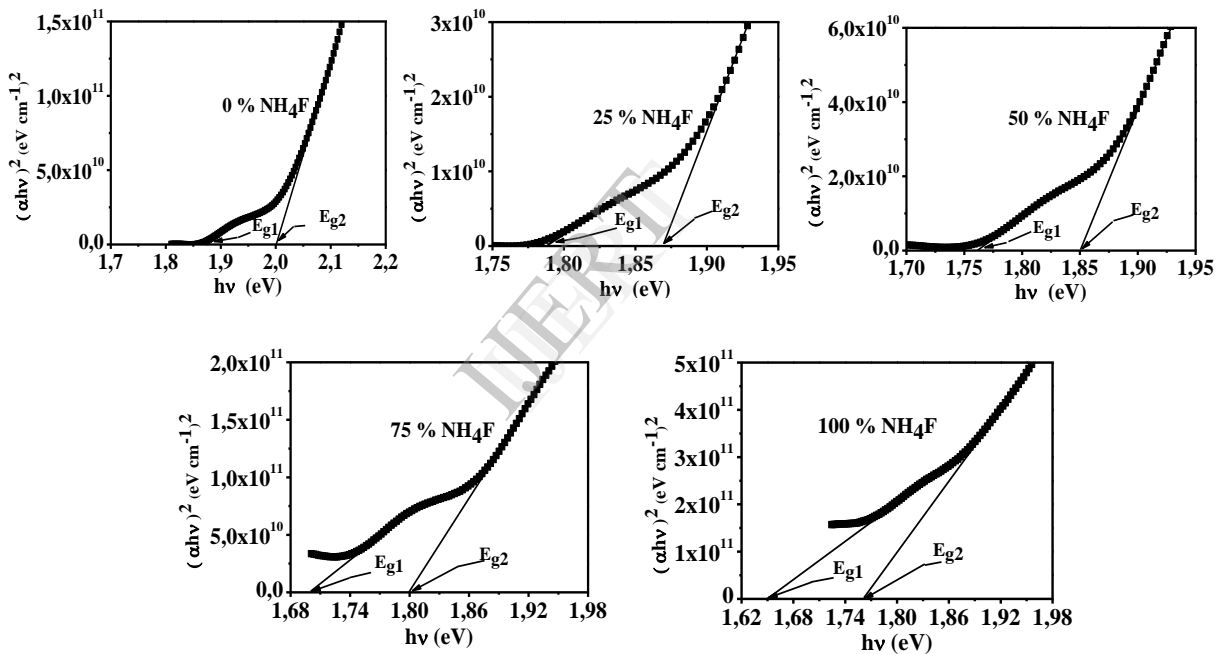


Figure 8 Relationship between $(\alpha h\nu)^2$ and photon energy of Sb_2S_3 thin films with different F⁻ % concentration.

The two allowed direct transitions E_{g1} and E_{g2} decrease from 1.86 to 1.65 eV and from 1.98 to 1.79 eV respectively with increasing the [F⁻] concentration (Figure 9 and Table 2). The band gap ($\approx 1.65\text{--}2$ eV) covers the maximum scan of the visible and near infrared ranges of the solar spectrum [17- 19].

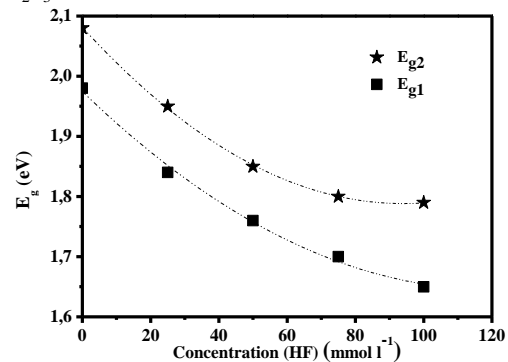


Figure 9. Direct energy gap E_g versus the F⁻ % concentration.

4. Conclusion

The effects of chemical etching of substrates on the structural and optical properties of Sb_2S_3 thin films were studied. It can be observed that the samples obtained after evaporation have an amorphous structure. We also note that the attacked Sb_2S_3 layers presented roughness more significant than those of the substrates attacked for the weak and average concentration of $[\text{F}^-]$, what it is conversely for the strong concentration. Only with average concentration the croissance of the Sb_2S_3 material achieves the texture of surface. Relatively high absorption coefficients between 10^4 cm^{-1} and 10^6 cm^{-1} were calculated. Two direct energy transitions which lie between 1.65–2.00 eV ranges were found. These characteristics reported in this work make the Sb_2S_3 a potential candidate as absorber material in solar cells applications.

5. References

- [1] K. Petkov, R. Todorov, D. Kozhuharova, L. Tichy, E. Cernoskova, P. J. S. Ewen, "Changes in the physicochemical and optical properties of chalcogenide thin films from the systems As-S and As-S-Tl", *J. Mat. Sci.* 39 (2004), pp. 961-968.
- [2] E. Marquez, A. M. Bernal-Oliva, J. M. Gonzales-Leal, R. Pietro-Alcon, T. Wagner, *J. Phys. D: Appl. Phys.* 39 (2006), pp. 1793-1798.
- [3] Q. Lu, H. Zeng, Z. Wang, X. Cao, L. Zhang, *Nanotechnology*, 17 (2006) 2098–2104.
- [4] Z. S. El Mandouh, S. N. Salama, *J. Mat. Sci.* 25 (1990), pp. 1715-1724.
- [5] M. Thamilselvan, K. Premnazeer, D. Mangalaraj, S. K. Narayandass, *physica B*, 337 (2003), pp. 404-410.
- [6] M. Parlak, A. F. Qasrawi, C. Ercelebi, *J. Mat. Sci.* 38 (2003), pp. 1507-1511.
- [7] J. D. Desai, C. D. Lokhande, *Thin Solid Films*, 237 (1994), pp. 29-31.
- [8] A. M. Salem, M. Soliman Selim, *J. Phys. D: Appl. Phys.* 34 (2001), pp. 12-17.
- [9] H. Chen, C. Zhu, F. Gan, *J. Sol-Gel Sci. Technol.* 12 (1999), pp. 181-187.
- [10] I. K. El Zawawi, A. Abdel-Moez, F. S. Terra, M. Mounir, *Thin Solid Films*, 334 (1998), pp. 300-304.
- [11] Z. S. El Mandouh, S. N. Salama, *J. Mat.Sci.* 25 (1990), pp. 1715-1724.
- [12] L. Kasturi, Chopra, "Thin Film Phenomena", McGraw-Hill Book Company, New York, 1969, p. 844.
- [13] T. Cormant, P. Enoksson, O. Stemme, *J. Micromech.* 8 (1998), pp. 84-87.
- [14] A. Richardt, A. M. Durand, *Journal of Comparative Physiology B*, 63 (1994), pp. 169-174.
- [15] M. Kanzari, B. Rezig, "Effect of deposition temperature on the optical and structural properties of as-deposited CuInS_2 films", *Semicond. Sci. Technol.* 15 (2000), pp. 335-340.
- [16] K. Tien, R. Ulrich, R. J. Martin, *Appl. Phys. Lett.* 14 (1969), pp. 291-294.
- [17] L. P. Deshmukh, S. G. Holikatti, B. P. Rane, B. M. More, P. P. Hankare, *J. Electrochem.Soc.* 41 (1994), pp. 1779-1783.

- [18] O. Savadogo, K. C. Manda, *Solar Energy Mater, Solar Cells* 26 (1992), pp. 117-136.
- [19] M. T. S. Nair, Y. Pena, J. Campos, V. M. Garica, P. K. Nair, *J. Electrochem. Soc.* 145 (1998), pp. 2113-2120.